ARTICLE

First-Principles Study on Electronic and Optical Properties of Graphene-Like Boron Phosphide Sheets

Shao-feng Wang[a], Xiao-jun Wu[a,b,c*]

a. CAS Key Laboratory of Materials for Energy Conversion and Department of Materials Science and Engineering, University of Science and Technology of China, Hefei 230026, China
b. Synergetic Innovation Center of Quantum Information & Quantum Physics, University of Science and Technology of China, Hefei 230026, China
c. School of Chemistry and Materials Science and Hefei National Laboratory for Physical Sciences at the Microscale, University of Science and Technology of China, Hefei 230026, China.

(Dated: Received on May 18, 2015; Accepted on June 16, 2015)

Two-dimensional semiconducting materials with moderate band gap and high carrier mobility have a wide range of applications for electronics and optoelectronics in nanoscale. On the basis of first-principles calculations, we perform a comprehensive study on the electronics and optical properties of graphene-like boron phosphide (BP) sheets. The global structure search and first-principles based molecular dynamic simulation indicate that two-dimensional BP sheet has a graphene-like global minimum structure with high stability. BP monolayer is semiconductor with a direct band gap of 1.37 eV, which reduces with the number of layers. Moreover, the band gaps of BP sheets are insensitive to the applied uniaxial strain. The calculated mobility of electrons in BP monolayer is as high as 10^6 cm^2/(V·s). Lastly, the MoS_2/BP van der Waals heterobilayers are investigated for photovoltaic applications, and their power conversion efficiencies are estimated to be in the range of 17.7%−19.7%. This study implies the potential applications of graphene-like BP sheets for electronic and optoelectronic devices in nanoscale.

Key words: Density functional theory, BP sheet, Electronic structure, Optical properties

I. INTRODUCTION

Two-dimensional (2D) materials with single-atomic thickness have attracted many research interests for their novel properties with respect to the bulk materials and great potential in electronics, optoelectronics, and energy applications [1−31]. In order to develop high-performance electronic and optoelectronic devices, *e.g.* field-effect transistor, it is essential that 2D materials have moderate band gap and high carrier mobility, as well as high thermal and chemical stability.

In the past years, graphene, as well as other group-IV element based 2D materials, has been investigated intensively for the massless carriers and extremely high carrier mobility, but the absence of band gap limits the applications [5−15]. In contrary, group III-V compound hexagona-boron nitride (h-BN) monolayer is a semiconductor with high thermal and chemical stability, but the band gap is as large as about 6 eV [16−20]. Transition metal dichalcogneides (TMDs) sheets have been considered very promising materials for their moderate band gap. For example, MoS_2 monolayer, a typical TMD material, is a direct-gap semiconductor with a moderate band gap of 1.57 eV [21−24]. However, its electronic structure is sensitive to the strain and number of layers, as well as the carrier mobility is only 200−500 cm^2/(V·s) [22, 25, 26]. Very recently, phosphorene has attracted substantial research interest for both moderate direct band gap of 1.51 eV and rather high hole-mobility of order 10^4 cm^2/(V·s) with distinct anisotropic transport properties [27−29], but the chemical reactivity of phosphorene in atmosphere and weak mechanical strength are technic hinders for its applications [27, 30, 31]. Therefore, exploring new 2D semiconducting materials for electronics and optoelectronics application is still a long-term target.

In this work, we perform a comprehensive theoretical study on group III-V compound boron phosphide (BP) multilayers with density functional theory method. Previous theoretical work has shown that graphene-like BP monolayer is semiconductor with a direct band gap ranging from 0.81 eV to 1.82 eV, which may be used to fabricate electronic device in nanoscale [20, 32−36]. Experimentally, BP films have been synthesized on silicon carbide by CVD method [37]. In this work, we show that BP monolayer has a graphene-like global minimum structure. Importantly, BP monolayer has a high electron mobility of 10^6 cm^2/(V·s) and strong optical abs-

*Author to whom correspondence should be addressed. E-mail: xjwu@ustc.edu.cn

orption from 1.37 eV to 4 eV. What's more, monolayer MoS_2/few-layer BP van der Waals heterojunctions have power conversion efficiencies in the range of 17.7% to 19.7%, suitable for optoelectronic applications.

II. METHOD

All calculations are performed with density functional theory (DFT) method implemented in VASP 5.2 software package [38]. The exchange-correlation energy is treated using the Perdew-Burke-Ernzerhof (PBE) functional, and the Grimme's DFT-D2 dispersion correlation [39] is applied to consider the long-range Var der Waals interactions in BP multilayers. Note that PBE functional tends to underestimate the band gap of semiconductors, the screened hybrid HSE06 functional [40] is applied to calculate the electronic properties of BP sheets. The ion-electron interaction is treated with the projector-augment-wave (PAW) method. For geometrical optimization, both lattice constants and atomic positions are relaxed until the total energy change is less than 1.0×10^{-5} eV, and the forces on the atoms are all less than 0.01 eV/Å. The energy cutoff for the plane-wave basis is set to 500 eV. A vacuum space of ∼20 Å along the direction normal to the 2D BP plane is used to ensure the interlayer interaction generated by the periodic boundary condition can be neglected. The first Brillouin zone is sampled with k-meshes of 12×12×1 and 12×12×12 for graphene-like BN monolayer and bulk. The constant temperature and constant volume quantum BOMD simulation is performed by using the Nosé-Hoover method, in which the kinetic energy fluctuation of the thermostat variable is controlled by coupling it to another thermostat variable and the temperature of the system is maintained at 2500 K [41, 42]. The time step is 1.0 fs and the total simulation time is 5.0 ps. The global structure search is performed with the particle-swarm optimization (PSO) method within the evolutionary algorithm, as implemented in CALYPSO code [43]. The population size is set to 50, and the number of generations is maintained to be 30. The required structure relaxations are performed using the PBE functional, as implemented in VASP 5.2. The optical absorption coefficient are calculated by the dielectric function using the following expression

$$\alpha(\omega) = \frac{\omega\varepsilon_2}{cn} \tag{1}$$

$$n = \sqrt{\frac{\sqrt{\varepsilon_1^2+\varepsilon_2^2}+\varepsilon_1}{2}} \tag{2}$$

where ω is the light frequency, n is the index of refraction, ε_1 and ε_2 are the real and imaginary parts of the dielectric function. To ensure the reliability of calculation, the optical property computation is based on HSE06 results with a high dense sampling of K points.

III. RESULTS AND DISCUSSION

At first, the structural and electronic properties of BP bulk are studied to benchmark the calculations. The BP bulk has a zinc blende crystalline structure, as shown in Fig.1(a). The optimized lattice constant of BP bulk is 4.547 Å with PBE functional, agreeing well with the experimental results of 4.550 Å [44]. Then, the band structures of BP bulk are calculated with HSE06 method, as shown in Fig.2. The calculated band gap of BP bulk is 1.98 eV, which is consistent with the experimental value of 2.0±0.2 eV by ultra-soft-X-ray spectroscopy [45]. In the following calculations, the structures are optimized at PBE level and the electronic properties are studied at HSE06 level.

Previous theoretical studies have indicated that graphene-like BP monolayer is stable, but it is a question whether this structure is a global minimum. Thus, a global minimum structure search is performed at first on BP monolayer to explore its possible stable 2D structures. The calculated results show that the global minimum structure of BP monolayer is graphene like with a uniform distribution of B and P, as shown in Fig.1(b). The calculated B−P bond length in BP monolayer is 1.855 Å, which is slightly shorter than that in the bulk BP (1.969 Å), indicating a strengthened bonding between B and P atoms. To check the structure stability of BP monolayer, a BOMD simulation is performed at a high temperature of 2500 K for 5 ps. The simulation indicates that B−P bonds are reserved in the simulation timescale, indicating the high thermal stability of BP monolayer.

To determine the stabilization of the number of layers for 2D BP stripped from the bulk BP, the cleavage energies of BP ultrathin films with zinc-blende or graphene-like structures are calculated by subtracting the energies of BP ultrathin films from BP bulk energy with the same number of atoms, and further divided by the two surfaces area created after optimization. This method has been applied to AlN, BeO, GaN, SiC, ZnS, and ZnO systems [46]. Table I lists the calculated cleavage energies for BP ultrathin films. In which the whitespace denotes that the $2n$ layers of polar (111) or unpolar (110) surfaces are optimized to be n layers of graphene-like

TABLE I The cleavage energies of zinc-blende type BP ultrathin films with either polar (111) or unpolar (110) surfaces, and graphene-like BP layers are calculated.

Number of layers	Energy/(J/m^2)		
	(111)	(110)	Graphene-like
2			1.85
3		2.39	2.70
4		2.26	3.55
6	2.67	2.28	5.27
8	2.82	2.32	6.97

DOI:10.1063/1674-0068/28/cjcp1505100

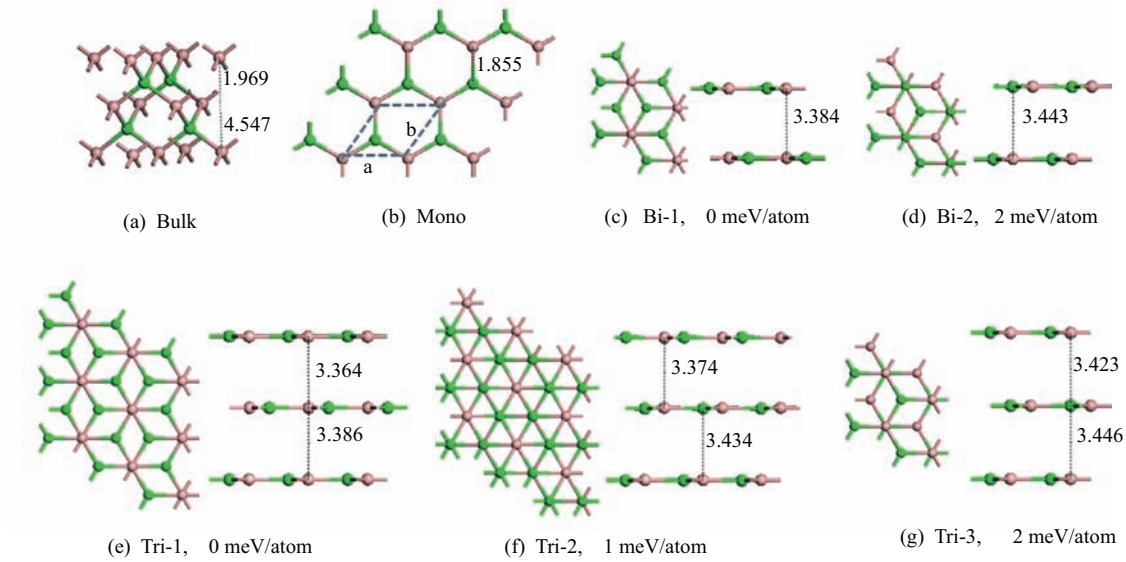

FIG. 1 The optimized structures of (a) BP bulk, (b) BP monolayer, (c) and (d) BP bilayer with AA and AB stacking, respectively, and (e)−(g) BP triple-layers with AAA, AAB and ABA stacking, respectively. Pink and blue ball denote boron and phosphorus atom, respectively.

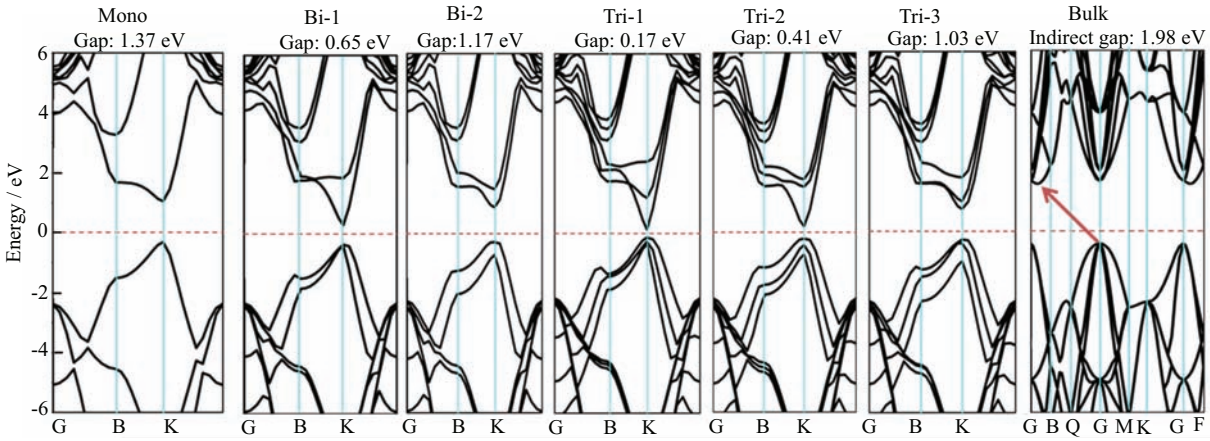

FIG. 2 The calculated electronic band structures of graphene-like BP monolayer, bilayer (Bi-1 and Bi-2) and tri-layer (Tri-1, Tri-2, and Tri-3), and zinc blende bulk BP.

structures spontaneously, which means that we should use the cleavage energies of $2n$ layers zinc-blende ultrathin films to compare with that of n layers graphene-like ultrathin films. For graphene-like BP layers, the cleavage energy increases linearly with the number of layers, however, for zinc-blende films (both polar (111) and unpolar (110) surfaces), the cleavage energy has little change. What's more, when the number of graphene-like layers up to 2 and 3, the graphene-like structure has a lower cleavage energy than the unpolar (110) and polar (111) surfaces, respectively, indicating the graphene-like BP bilayer or trilayer may be easily realized in experiment.

To study the structures of graphene-like BP bilayer, we construct five different configurations based on the relative position between the two layers. According to the energies, we choose the two most stable configurations (Bi-1 and Bi-2), as shown in Fig.1 (c) and (d). Based on two bilayer structures, we construct three most stable graphene-like BP tri-layers (Tri-1, Tri-2, and Tri-3) shown in Fig.1 (e) to (g). For the graphene-like BP bilayers, the most stable configuration is AA stacking, which is slightly more stable than AB stacking with the energy difference of 2 meV/atom. Similar behavior can be found in graphene-like BP tri-layers, where the most stable configuration is AAA stacking. The optimized interlayer distances range from 3.38 Å to 3.44 Å.

Figure 2 displays the calculated electronic band structures of BP bulk and graphene-like BP layers. BP bulk is a semiconductor with an indirect band gap of 1.98 eV, but BP monolayer is a direct-gap semiconductor with

DOI:10.1063/1674-0068/28/cjcp1505100

the band gap of 1.37 eV at HSE06 level. Interestingly, the band gap of BP layers depends on both the number of layers and their stacking modes. For example, the BP bilayer with AA stacking has a band gap of 0.65 eV, which is decreased compared with BP monolayer. Moreover, the BP bilayer with AB stacking has a band gap of 1.17 eV, which is larger than that of BP bilayer with AA stacking. Similar behavior can be found in BP trilayers. The BP trilayer with AAA stacking has the narrowest band gap of 0.17 eV, but the band gaps of BP trilayers with AAB and ABA stacking are 0.41 and 1.03 eV. From Fig.2, it can be found the band gap reduction of BP mulitlayers mainly results from the sharpening of CBM, whereas the profile of VBM doesn't change significantly. The density of states analysis results indicate that the CBM is mainly contributed by B's p_z orbitals, whereas the VBM is mainly contributed by P's p_z orbitals. It is supposed that the interlayer interaction between B's p_z orbitals results in the sharpening of CBM, which leads a significant reduction of band gap compared with BP monolayer.

Considering the shape profiles of CBM and VBM in graphene-like BP monolayer, the carrier mobility is calculated for both electron and hole with a phonon-limited scattering model, in which the scattering due to phonons is considered to be the primary mechanism limiting carrier mobility [47, 48]. In 2D materials, the carrier mobility is given by the following equation [29, 47−50].

$$\mu_{2\mathrm{D}} = \frac{e\hbar^3 C_{2\mathrm{D}}}{k_{\mathrm{B}} T m_e^* m_{\mathrm{d}} (E_1^i)^2} \tag{3}$$

where m^* is the effective mass and $m_{\mathrm{d}}=\sqrt{m_x^* m_y^*}$ is the average effective mass. E_1 represents the deformation potential constant of CBM for electron of VBM for hole along the transport direction, defined by the following equation:

$$E_1^i = \frac{\Delta V_i}{\Delta l / l_0} \tag{4}$$

where ΔV_i is the energy change of the i-th band under proper cell dilatation and compression (calculated with a step of 0.5%), l_0 is the lattice constant in the transport direction and Δl is the deformation of l_0. The elastic modulus $C_{2\mathrm{D}}$ in the transport direction is calculated from:

$$\frac{E - E_0}{S_0} = \frac{C_{2\mathrm{D}}}{2}\left(\frac{\Delta l}{l_0}\right)^2 \tag{5}$$

where E is the total energy and S_0 is the lattice volume at equilibrium for a 2D system. The temperature is set as 300 K. Here, both the carrier mobilities along x and y directions are studied.

For BP monolayer, the calculated electron mobility along x and y directions reach 3.00×10^6 and 1.14×10^5 $\mathrm{cm^2/(V\cdot s)}$, respectively. For BP bilayer and trilayer, the calculated electron mobilities reach as high as 2.72×10^7 and 8.60×10^7 $\mathrm{cm^2/(V\cdot s)}$ for x direction, respectively. For y directions, these values are 3.14×10^5 and 4.41×10^5 $\mathrm{cm^2/(V\cdot s)}$), respectively. These values are 10−100 times higher than that of graphene (of order 10^5 $\mathrm{cm^2/(V\cdot s)}$) [51]. However, the hole mobilities of BP layers are much smaller than that of electron mobility. The calculated hole mobilities for BP monolayer, bilayer and trilayer are 0.87×10^4, 0.72×10^4, and 0.59×10^4 $\mathrm{cm^2/(V\cdot s)}$ for x direction, respectively. For y direction, these values are 1.70×10^4, 0.50×10^4, and 3.62×10^4 $\mathrm{cm^2/(V\cdot s)}$, respectively. These values are comparable to the hole mobility of phosphorene monolayer, which is 1.44×10^4 $\mathrm{cm^2/(V\cdot s)}$ calculated with same method, agreeing well with the experiment results of 10000−26000 $\mathrm{cm^2/(V\cdot s)}$ reported recently [29].

With a moderate direct band gap and ultra-high carrier mobility, one potential application of BP layers is for photovoltaic application. Based on HSE06 calculations, the computed VBM levels are −5.33, −5.26, and −5.15 eV, while the CBM levels are −3.96, −4.09 and −4.12 eV for BP monolayer, bilayer and trilayer, respectively. For MoS_2 monolayer, the computed VBM and CBM levels are −6.37 and −4.23 eV, respectively, which match those of BP layers very well, giving a type-II alignment with both materials [52, 53], as shown in Fig.3(a). Thus, a potential solar-cell device made of BP layers and MoS_2 monolayer is constructed by forming MoS_2/graphene-like BP layers van der Waals heterojunctions. The computed optical absorption spectra of BP layers are plotted in Fig.3(b). We can see the optical adsorption is fairly strong over a wide energy range between 1.37 and 4 eV, a range important for enhancing efficiency of a solar cell. Further, the upper limit of the power conversion efficiency (PCE) η is estimated in the limit of 100% external quantum efficiency (EQE) with

$$\begin{aligned}\eta &= \frac{J_{\mathrm{sc}} V_{\mathrm{oc}} \beta_{\mathrm{FF}}}{P_{\mathrm{solar}}} \\ &= (0.65 E_{\mathrm{g}}^{\mathrm{d}} - \Delta E_{\mathrm{c}} - 0.3) \cdot \\ &\quad \frac{\int_{E_{\mathrm{g}}^{\mathrm{d}}}^{\infty} \frac{P(\hbar\omega)}{\hbar\omega} \mathrm{d}(\hbar\omega)}{\int_0^{\infty} P(\hbar\omega) \mathrm{d}(\hbar\omega)}\end{aligned} \tag{6}$$

where 0.65 is the fill factor (FF), $P(\hbar\omega)$ is the AM1.5 solar energy flux (expressed in $\mathrm{W/(m^2\cdot eV)}$ at the photon energy, and $E_{\mathrm{g}}^{\mathrm{d}}$ is the band gap of the donor, the $(E_{\mathrm{g}}^{\mathrm{d}}-\Delta E_{\mathrm{c}}-0.3)$ term is an estimation of the maximum open circuit voltage. The integral in the numerator is the short circuit current J_{sc} under the limit of 100% EQE, and the integral in the denominator is the integrated AM1.5 solar flux. Figure 3(c) shows solar systems constructed with Mono/Bi-2/Tri-3 and monolayer MoS_2 can get PECs as high as ∼17.7%/19.7%/18.8%. These values are comparable to that of the recent predicted bilayer phosphorene/monolayer MoS_2 sys-

DOI:10.1063/1674-0068/28/cjcp1505100

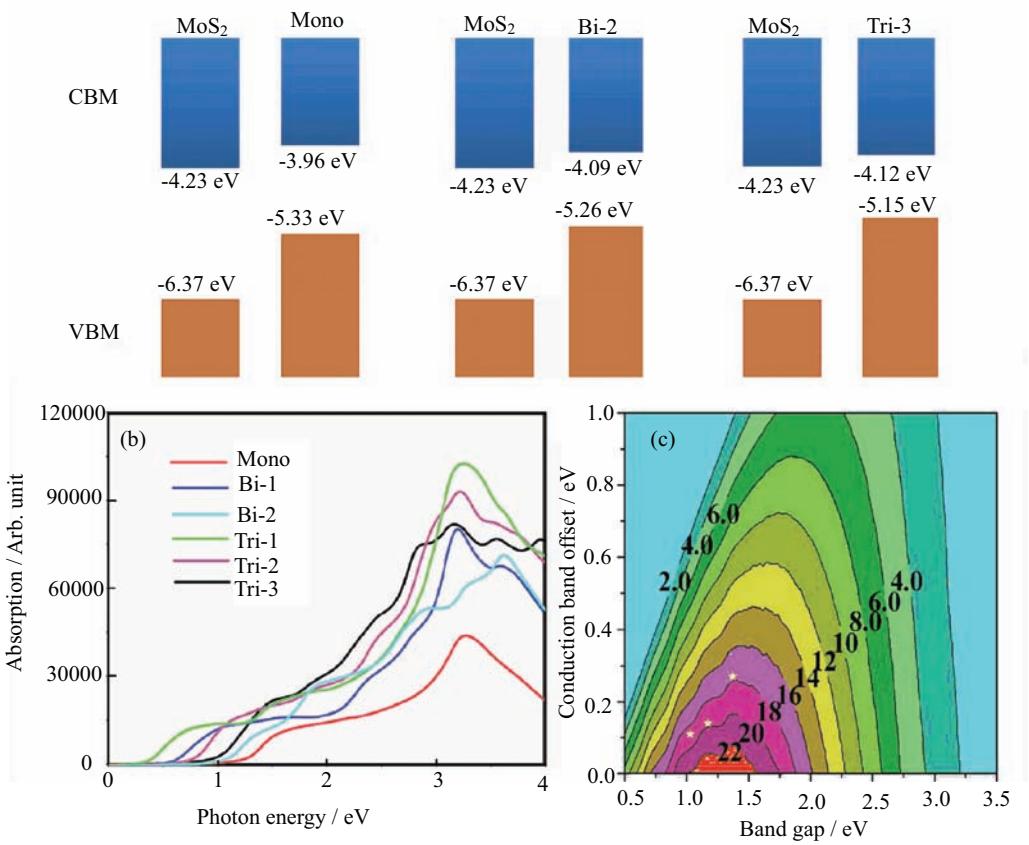

FIG. 3 (a) The band alignment of MoS_2/BP van der Waals heterojunctions. (b) The optical absorption spectra of BP layers. (c) The computed PCE as a function of donor band gap and conduction band offset.

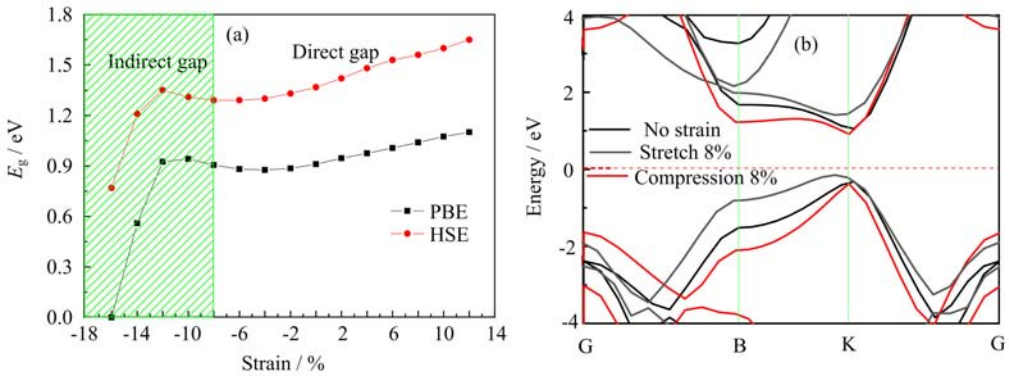

FIG. 4 (a) The band gap and (b) band structures of BP monolayer under a uniaxial strain.

tems (16%−18%) [54] and the PCBM/CBN system (10%−20%) [55].

Although the newly MoS_2/BP layers show intriguing properties for potential applications in solar cells, the chemical stability and strain effect on band gap are also important for their practical applications. At first, the effect of strain on band gap are investigated. Figure 4(a) displays the band gap of BP monolayer with a uniaxial deformation in the range of −12% to 12% (PBE and HSE06). The variation tendency of HSE06 results are in accord with PBE results. We can see that the strain has weak influence on the change of the band gap. Especially for strain from compression 8% to stretch 8%, the change of direct band gap is very small just from −0.08 eV to 0.19 eV based on the band gap of monolayer BP. Moreover, the band structures near VBM and CBM changes slightly, indicating that the carrier mobility almost unchanged. Thus, MoS_2/BP heterojunctions are robust for a slightly uniaxial deformation. Further, to investigate the chemical stability when the device works in environment, the adsorption of gas molecules, such as N_2, O_2, H_2O, H_2,

DOI:10.1063/1674-0068/28/cjcp1505100

and CO_2, on BP monolayer is studied. We find that the minimum distance between gas moleculars (N_2, O_2, H_2O, H_2, and CO_2) and BP monolayer are 3.96, 3.46, 3.36, 3.66, and 3.84 Å, respectively. Absorption energies for different gas moleculars on the surface of BP monolayer are also calculated, which is defined by $E_{ad}=E_{gas}-E_{BP}-E_{gas@BP}$, where $E_{gas@BP}$ means the total energy of gas molecular adsorption on the BP monolayer, E_{gas} and E_{BP} are the energy of gas molecular and BP monolayer, respectively. We get the adsorption energies for N_2, O_2, H_2O, H_2, and CO_2 are 0.009, 0.008, 0.026, 0.010, and 0.014 eV, respectively. The calculated results show that these gas molecules physically adsorb on BP monolayer, indicate that performance of MoS_2/BP layers are not affected by the gas molecules in environment.

IV. CONCLUSION

We have performed a comprehensive study on the electronic, optical, and mechanical properties of graphene-like BP layers. With the global structure search, we show that BP monolayer has a graphene-like global minimum structure. The BP monolayer is a semiconductor with a direct band gap of 1.37 eV. By increasing the number of layers, the band gap of BP few layers decreases sharply. The calculated mobility of electrons in BP monolayer is as high as 10^6 $cm^2/(V{\cdot}s)$. The MoS_2/BP van der Waals heterobilayers are investigated for photovoltaic applications, and their power conversion efficiencies are estimated to be in the range of 17.7% to 19.7%. Our studies suggest that graphene-like BP layers are very promising candidate materials for future applications in optoelectronics and electronics.

V. ACKNOWLEDGMENTS

This work was supported by the National Key Basic Research Special Foundation of China (No.2011CB921400 and No.2012CB922001), the National Natural Science Foundation of China (No.51172223 and No.21421063), the Strategic Priority Research Program of Chinese Academy of Science (No.XDB01020300), the One-Hundred Talent Project of Chinese Academy of Science, the Fundamental Research Funds for the Central Universities (No.WK2060190025 and No.WK2060140014), the National Outstanding Young Talent Program of China and the Shanghai Supercomputer Center and Supercomputing Center of USTC.

[1] R. Fivaz and E. Mooser, Phys. Rev. **163**, 743 (1967).
[2] E. H. Hwang and S. Das Sarma, Phys. Rev. B **77**, 115449 (2008).
[3] A. K. Geim and I. V. Grigorieva, Nature **499**, 419 (2013).
[4] B. Radisavljevic, A. Radenovic, J. Brivio, V. Giacometti, and A. Kis, Nature Nanotech. **6**, 147 (2011).
[5] K. S. Novoselov, A. K. Geim, S. V. Morozov, D. Jiang, Y. Zhang, S. V. Dubonos, I. V. Grigorieva, and A. A. Firsov, Science **306**, 666 (2004).
[6] M. Houssa, G. Pourtois, M. M. Heyns, V. V. Afanas'ev, and A. Stesmans, Phys. Tech. High-K Mater. **33**, 185 (2010).
[7] B. Lalmi, H. Oughaddou, H. Enriquez, A. Kara, S. Vizzini, B. Ealet, and B. Aufray, Appl. Phys. Lett. **97**, 223109 (2010).
[8] E. Bianco, S. Butler, S. Jiang, O. D. Restrepo, W. Windl, and J. E. Goldberger, ACS Nano **7**, 4414 (2013).
[9] K. S. Novoselov, Z. Jiang, Y. Zhang, S. V. Morozov, H. L.Stormer, U. Zeitler, J. C. Maan, G. S. Boebinger, P. Kim, and A. K. Geim, Science **315**, 1379 (2007).
[10] C. Lee, X. Wei, J. W. Kysar, and J. Hone, Science **321**, 385 (2008).
[11] J. H. Seol, I. Jo, A. L. Moore, L. Lindsay, Z. H. Aitken, M. T. Pettes, X. Li, Z. Yao, R. Huang, D. Broido, N. Minqo, R. S. Ruoff, and L. Shi, Science **328**, 213 (2010).
[12] Z. Ni, Q. Liu, K. Tang, J. Zheng, J. Zhou, R. Qin, Z. Gao, D. Yu, and J. Lu, Nano Lett. **12**, 113 (2012).
[13] L. Liao, Y. C. Lin, M. Bao, R. Cheng, J. Bai, Y. Liu, Y. Qu, K. L. Wang, Y. Huang, and X. Duan, Nature **467**, 305 (2010).
[14] N. J. Roome and J. D. Carey, ACS Appl. Mater. Inter. **6**, 7743 (2014).
[15] A. H. Castro Neto, F. Guinea, N. M. R. Peres, K. S. Novoselov, and A. K. Geim, Rev. Mod. Phys. **81**, 109 (2009).
[16] C. Zhi, Y. Bando, C. Tang, H. Kuwahara, and D. Golberg, Adv. Mater. **21**, 2889 (2009).
[17] A. Nag, K. Raidongia, K. P. S. S. Hembram, R. Datta, U. V. Waghmare, and C. N. R. Rao, ACS Nano **4**, 1539 (2010).
[18] E. Hernández, C. Goze, P. Bernier, and A. Rubio, Phys. Rev. Lett. **80**, 4502 (1998).
[19] A. P. Suryavanshi, M. F. Yu, J. Wen, C. Tang, and Y. Bando, Appl. Phys. Lett. **84**, 2527 (2004).
[20] H. Şahin, S. Cahangirov, M. Topsakal, E. Bekaroglu, E. Akturk, R. Senger, and S. Ciraci, Phys. Rev. B **80**, 155453 (2009).
[21] K. F. Mak, C. Lee, J. Hone, J. Shan, and T. F. Heinz, Phys. Rev. Lett. **105**, 136805 (2010).
[22] B. Radisavljevic, A. Radenovic, J. Brivio, V. Giacometti, and A. Kis, Nature Nanotech. **6**, 147 (2011).
[23] Q. H. Wang, K. Kalantar Zadeh, A. Kis, J. N. Coleman, and M. S. Strano, Nature Nanotech. **7**, 699 (2012).
[24] H. Shi, H. Pan, Y. W. Zhang, and B. I. Yakobson, Phys. Rev. B **87**, 155304 (2013).
[25] Q. Yue, J. Kang, Z. Shao, X. Zhang, S. Chang, G. Wang, S. Qin, and J. Li, Phys. Lett. A **376**, 1166 (2012).
[26] R. Fivaz and E. Mooser, Phys. Rev. **163**, 743 (1967).
[27] L. Kou, T. Frauenheim, and C. Chen, J. Phys. Chem. Lett. **5**, 2675 (2014).
[28] L. Li, Y. Yu, G. J. Ye, Q. Ge, X. Ou, H. Wu, D. Feng, X. H. Chen, and Y. Zhang, Nature Nanotech. **9**, 372 (2014).
[29] J. S. Qiao, X. Kong, Z. X. Hu, F. Yang, and W. Ji,

DOI:10.1063/1674-0068/28/cjcp1505100

Nature Commun. **5**, 4475 (2014).
[30] Q. Wei and X. Peng, Appl. Phys. Lett. **104**, 251915 (2014).
[31] A. S. Rodin, A. Carvalho, and A. H. Castro Neto, Phys. Rev. Lett. **112**, 176801 (2014).
[32] A. López-Castillo, Int. J. Quant. Chem. **112**, 3152 (2012).
[33] Y. Wang and S. Shi, Solid State Comm. **150**, 1473 (2010).
[34] M. Wu, X. Wu, Y. Pei, and X. Zeng, Nano Res. **4**, 233 (2011).
[35] Z. Sohbatzadeh, M. R. Roknabadi, N. Shahtahmasebi, and M. Behdani, Phys. E-Low-Dimensional Systems & Nanostructures **65**, 61 (2015).
[36] J. Dong, H. Li, and L. Li, NPG Asia Mater **5**, e56 (2013).
[37] G. Li, J. K. C. Abbott, J. D. Brasfield, P. Liu, A. Dale, G. Duscher, P. D. Rack, and C. S. Feigerle, Appl. Surf. Sci. **327**, 7 (2015).
[38] G. Kresse and J. Furthmüller, Phys. Rev. B **54**, 11169 (1996).
[39] S. Grimme, J. Comput. Chem. **27**, 1787 (2006).
[40] J. Heyd, G. E. Scuseria, and M. Ernzerhof, J. Chem. Phys. **118**, 8207 (2003).
[41] B. Delley, J. Chem. Phys. **113**, 7756 (2000).
[42] G. J. Martyna, M. L. Klein, and M. Tuckerman, J. Chem. Phys. **97**, 2635 (1992).
[43] Y. Wang, J. Lv, L. Zhu, and Y. Ma, Phys. Rev. B **82**, 094116 (2010).
[44] P. Popper and T. A. Ingles, Nature **179**, 1075 (1957).
[45] V. A. Fomichev, I. I. Zhukova, and I. K. Polushin, J. Phys. Chem. Solids **29**, 1025 (1968).
[46] C. Freeman, F. Claeyssens, N. Allan, and J. Harding, Phys. Rev. Lett. **96**, 066102 (2006).
[47] S. Takagi, A. Toriumi, M. Iwase, and H. Tango, Electron Devices, IEEE Transactions on **41**, 2357 (1994).
[48] W. Walukiewicz, H. E. Ruda, J. Lagowski, and H. C. Gatos, Phys. Rev. B **30**, 4571 (1984).
[49] J. Bardeen and W. Shockley, Phys. Rev. **80**, 72 (1950).
[50] J. Xi, M. Long, L. Tang, D. Wang, and Z. Shuai, Nanoscale **4**, 4348 (2012).
[51] J. Chen, J. Xi, D. Wang, and Z. Shuai, J. Phys. Chem. Lett. **4**, 1443 (2013).
[52] M. C. Scharber, D. Wuhlbacher, M. Koppe, P. Denk, C. Waldauf, A. J. Heeger, and C. L. Brabec, Adv. Mater. **18**, 789 (2006).
[53] J. D. Servaites, M. A. Ratner, and T. J. Marksb, Appl. Phys. Lett. **95**, 163302 (2009).
[54] J. Dai and X. C. Zeng, J. Phys. Chem. Lett. **5**, 1289 (2014).
[55] N. Lu, H. Guo, L. Li, J. Dai, L. Wang, W. N. Mei, X. Wu, and X. C. Zeng, Nanoscale **6**, 2879 (2014).

DOI:10.1063/1674-0068/28/cjcp1505100